Appl. Phys. A (2015) 120:1573–1578
DOI 10.1007/s00339-015-9357-z

Applied Physics A
Materials Science & Processing

Transport critical current density of $(Bi_{1.6}Pb_{0.4})Sr_2Ca_2Cu_3O_{10}/Ag$ superconductor tapes with addition of nanosized $CoFe_2O_4$

M. Hafiz[1] · R. Abd-Shukor[1]

Received: 4 February 2015 / Accepted: 8 July 2015 / Published online: 17 July 2015

Abstract The effect of nanosized $CoFe_2O_4$ (60 nm) addition on the transport critical current density, J_c, of $(Bi_{1.6}Pb_{0.4})Sr_2Ca_2Cu_3O_{10}(CoFe_2O_4)_x$ ($x = 0$–0.05 wt%) superconductor prepared by the co-precipitation method was investigated. The optimal J_c (measured using the four-point probe method) was observed in the $x = 0.01$ wt% pellets. Using this optimal wt%, Ag-sheathed $(Bi_{1.6}Pb_{0.4})$-$Sr_2Ca_2Cu3O_{10}(CoFe_2O_4)_{0.01}$ superconductor tapes were fabricated using the powder-in-tube method. The tapes were sintered for 50 and 100 h at 845 °C. The phase and microstructure of the samples were determined using the powder X-ray diffraction method and scanning electron microscopy, respectively. The temperature dependence of J_c for the tapes in various applied magnetic fields was also measured. J_c of $(Bi_{1.6}Pb_{0.4})Sr_2Ca_2Cu_3O_{10}(CoFe_2O_4)_{0.01}/Ag$ tapes sintered for 100 h was 22,420 A/cm^2 at 30 K. The non-added tapes sintered for 100 h showed a much lower J_c (8280 A/cm^2 at 30 K). This study showed that addition of $CoFe_2O_4$ nanoparticles enhanced the transport critical current density in the $(Bi_{1.6}Pb_{0.4})Sr_2Ca_2Cu_3O_{10}$ superconductor tapes. This result is consistent with the previous calculations on frozen flux superconductor in a nanomagnet–superconductor hybrid system.

1 Introduction

The $Bi_{1.4}Pb_{0.6}Sr_2Ca_2Cu_3O_{10+\delta}$ (Bi-2223) high-temperature superconductor has great potentials to be developed for energy applications. However, the flux pinning capability and intergrain connectivity need to be improved in order to overcome the rapid decrease in the transport critical current density, J_c, at high temperatures and in magnetic fields [1, 2].

Nanoparticles have been added to Bi-2223 superconductor to act as pinning centers in order to improve flux pinning ability [3–6]. Nanosized Al_2O_3 (50 nm) improved J_c of Bi-2223 pellets by 30 % with 0.2 wt% addition [4]. It also improved the J_c in applied magnetic fields. Ag_2CO_3 addition increases the critical current density of Bi-2223 pellets by more than three times with 25 wt% addition [6].

Nanoparticles with size larger than the coherence length, ξ, and smaller than penetration depth, λ, have been suggested to increase J_c [7]. However, other studies showed that the optimum size of pinning centers should be comparable to λ rather than ξ [8]. The coherence length of Bi-2223 is around 2.9 nm, and the penetration depth is between 60 and 1000 nm [9]. Stronger interaction between the nanoparticles and flux lines leading to higher J_c can be expected for nanoparticles with size d, where $\xi < d < \lambda$ [10].

The average size of $CoFe_2O_4$ nanoparticles employed in this study was 60 nm. $CoFe_2O_4$ was selected in this study because the average size is comparable with the penetration depth of Bi-2223 which is within the range required in the frozen flux model as discussed in [10] where enhanced flux pinning can be expected. The frozen flux model also requires magnetic nanoparticles as the pinning center; hence, $CoFe_2O_4$ was chosen to enhance J_c in the Bi-2223 tapes. $CoFe_2O_4$ nanoparticles have spinel crystal structure, and the Néel temperature varies depending on the nanoparticle size ranging from 709 K (8 nm) to 809 K (92 nm) [11]. In this paper, we report the effect of $CoFe_2O_4$ on the transport critical current density, phase formation and microstructure of Ag-sheathed Bi-2223 tapes.

✉ R. Abd-Shukor
ras@ukm.edu.my

[1] School of Applied Physics, Universiti Kebangsaan Malaysia, 43600 Bangi, Selangor, Malaysia

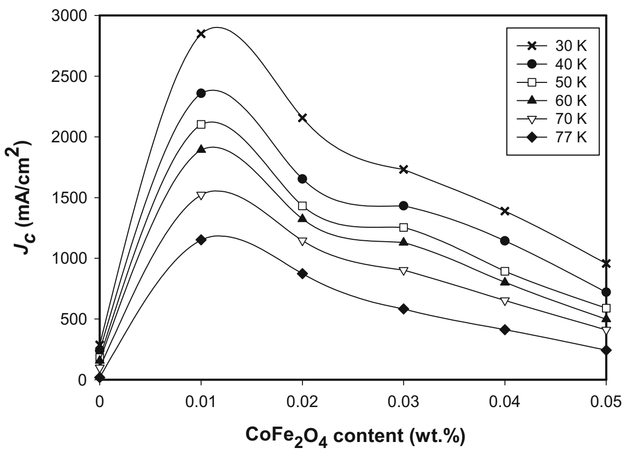

Fig. 1 Critical current density J_c of Bi-2223 in pellet form as a function of wt% $CoFe_2O_4$ content for temperatures between 30 and 77 K

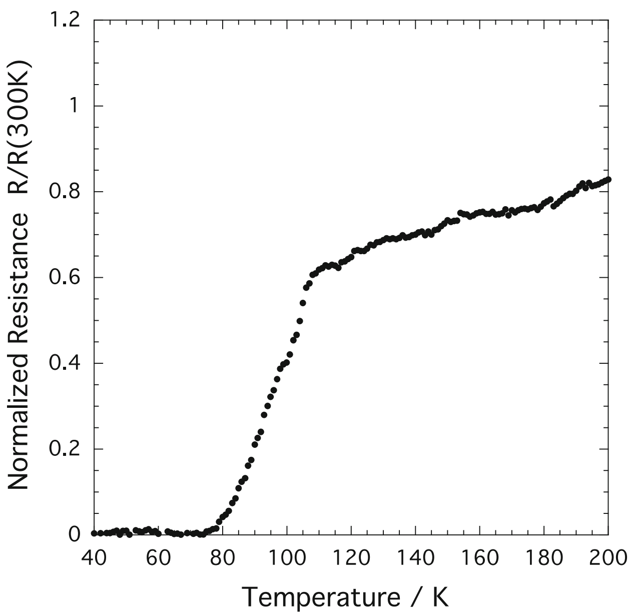

Fig. 2 Normalized temperature dependence of resistance for $CoFe_2O_4$-added Bi-2223 tape sintered for 100 h

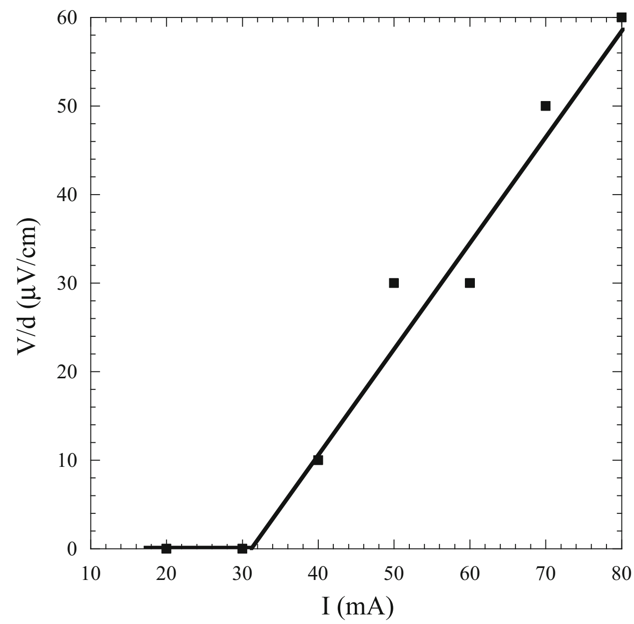

Fig. 3 I–V curve at 30 K for $CoFe_2O_4$-added Bi-2223 tape sintered for 100 h. *Black solid line* is used to determine J_c using the 1 μV/cm criterion

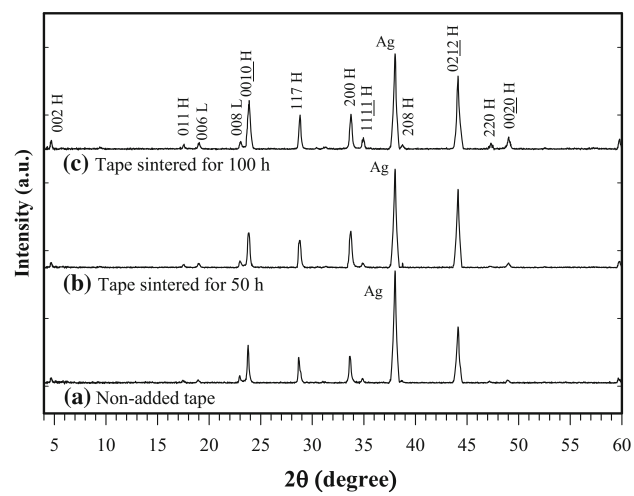

Fig. 4 XRD patterns of (*a*) non-added and $CoFe_2O_4$ nanoparticles-added tapes sintered for (*b*) 50 and (*c*) 100 h. (*H*) denotes the high-T_c phase (Bi-2223) and (*L*) denotes the low-T_c phase (Bi-2212)

2 Experimental details

$Bi_{1.4}Pb_{0.6}Sr_2Ca_2Cu_3O_{10}$ $(CoFe_2O_4)_x$ ($x = 0.00$–0.05 wt%) pellets with nanosized $CoFe_2O_4$ addition (from Inframat Advanced Materials, 99.9 % purity) were prepared. The Bi-2223 powders were prepared using the acetate co-precipitation method [12]. The mixed powders were ground and pressed into pellets and sintered at 845 °C for 48 h. The sample with $x = 0.01$ wt% $CoFe_2O_4$ addition showed the highest J_c at 77 K. This composition was chosen to fabricate Ag-sheathed Bi-2223 tapes by the powder-in-tube method. Tapes without the addition of $CoFe_2O_4$ were also prepared for comparison. $(Bi_{1.6}Pb_{0.4})Sr_2Ca_2Cu_3O_{10}$ powders prepared by the co-precipitation method were added with 0.01 wt% nanosized $CoFe_2O_4$ before being packed into a 6.35-mm-outer diameter and 4.35-mm-inner diameter Ag tube (Alfa Aesar, 99.9 %). The tube was drawn to a 1-mm wire and then pressed into 0.12-mm-thick and 1.35-mm-wide tapes. The tapes were then cut into 2–3 cm sections and sintered for 50 and 100 h at 845 °C.

The phase of the samples was examined by X-ray powder diffraction (XRD) using a Bruker D8 Advance

Table 1 Volume fraction and critical current density of $x = 0$ and $x = 0.01$ wt% of 60 nm $CoFe_2O_4$ nanoparticles-added Bi-2223 tapes sintered for 50 and 100 h at 30 and 77 K

X (wt. %)	Sintering time (h)	Volume fraction (%)		J_c (A/cm^2) (30 K)	J_c (A/cm^2) (77 K)
		Bi-2223	Bi-2212		
0.00	50	73	27	6370	1040
0.00	100	76	24	8280	1290
0.01	50	83	17	20,380	3860
0.01	100	86	14	22,420	4520

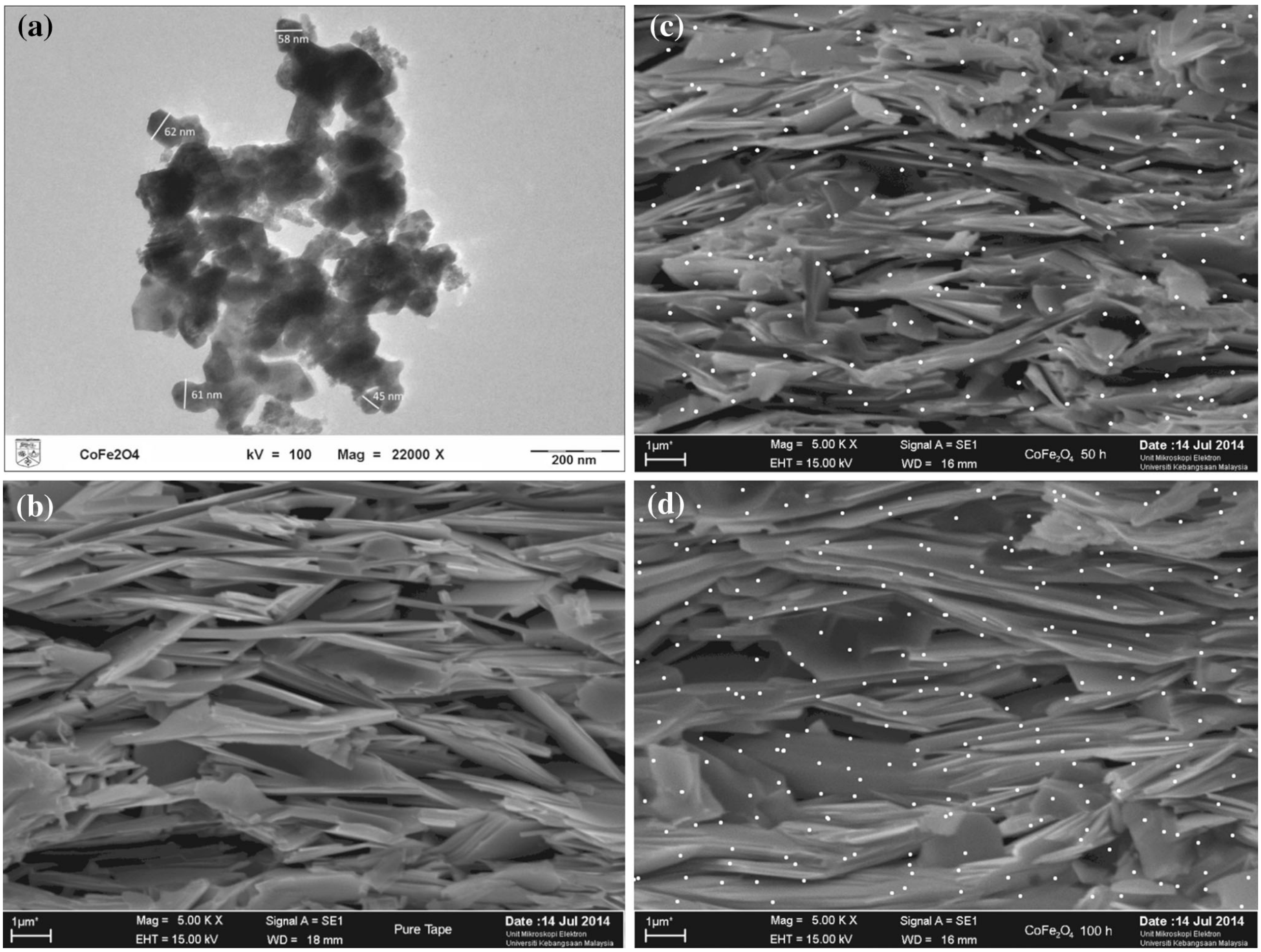

Fig. 5 Micrographs of **a** $CoFe_2O_4$ nanoparticles with an average size of 60 nm, **b** non-added Bi-2223 tape, **c** $CoFe_2O_4$-added Bi-2223 tape sintered for 50 h and **d** $CoFe_2O_4$-added Bi-2223 tape sintered for 100 h. *White dots* denote the distribution of $CoFe_2O_4$ nanoparticles in the tapes

diffractometer with CuK_α radiation. The microstructure of the tapes was examined using a Philips XL 30 scanning electron microscope (SEM). The distribution of $CoFe_2O_4$ in the tapes was determined using the energy-dispersive X-ray spectroscopy (EDX). A transmission electron microscope (TEM) using Philips model CM12 was used to confirm the average size of $CoFe_2O_4$ nanoparticles. The four-point probe method using the 1 V/cm criterion was used to determine J_c. The measurements were taken from 30 to 77 K in zero magnetic fields, and at 77 K under magnetic fields applied from 0 to 0.75 T.

3 Results and discussion

Figure 1 shows the J_c of $Bi_{1.4}Pb_{0.6}Sr_2Ca_2Cu_3O_{10}$ $(CoFe_2O_4)_x$ ($x = 0.00$–0.05 wt%) pellet between 30 and 77 K. The sample with $x = 0.01$ wt% of nanosized $CoFe_2O_4$ showed the highest J_c which was 2.85 A/cm^2 at 30 K and 1.15 A/cm^2 at 77 K. Therefore, this wt% of $CoFe_2O_4$ was used to prepare $Bi_{1.4}Pb_{0.6}Sr_2Ca_2Cu_3O_{10}$ $(CoFe_2O_4)_{0.01}$/Ag tape.

The onset transition temperature $T_{c\ onset}$ of the tapes with and without $CoFe_2O_4$ is around 110 K, and the zero

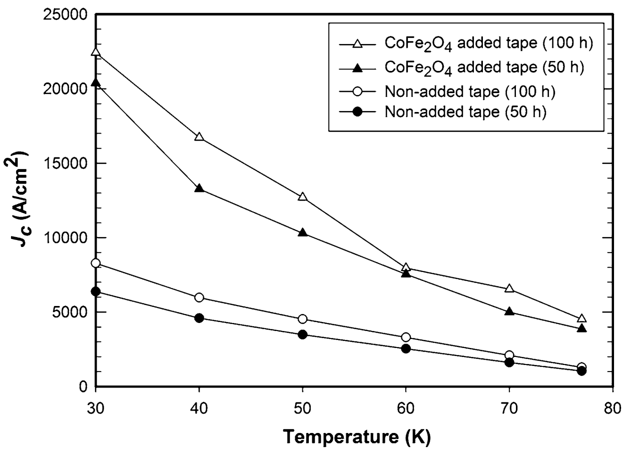

Fig. 6 Temperature dependence of critical current density J_c in zero magnetic field for non-added and $CoFe_2O_4$-added Bi-2223 tapes sintered for 50 and 100 h

resistance temperature $T_{c\ zero}$ is 78 K. Figure 2 shows the temperature dependence of resistance for $CoFe_2O_4$-added tape sintered for 100 h. The presence of Bi-2212 phase has resulted in a lower $T_{c\ zero}$ in the samples. The I–V curve for the same tape at 30 K is shown in Fig. 3.

The XRD pattern of the non-added tape is shown in Fig. 4a. Figure 4b shows the patterns for $x = 0.01$ wt% $CoFe_2O_4$-added tapes heated for 50 h, and Fig. 4c shows the pattern for $x = 0.01$ wt% $CoFe_2O_4$-added tapes heated for 100 h. Majority of the peaks in both non-added and nanosized $CoFe_2O_4$-added tapes correspond to the high-T_c Bi-2223 phase (H). A small number of peaks correspond to the low-T_c Bi-2212 phase (L) were also observed. The volume fraction of Bi-2223 phase was determined by

$$V_{2223} = \frac{\sum I_{2223}}{\sum I_{2223} + \sum I_{2212}}$$

where $\sum I_{2223}$ and $\sum I_{2212}$ are the sum of intensities of Bi-2223 and Bi-2212 phases, respectively [13, 14]. The tape sintered at 100 h showed the highest volume fraction of Bi-2223 (Table 1). No Bi-2201 peaks were observed.

TEM micrograph showed that the average grain size of $CoFe_2O_4$ nanoparticles used in this study was about 60 nm (Fig. 5a). This size is larger than the coherence length, ξ, and comparable to the penetration depth, λ, of Bi-2223. SEM micrographs of the non-added and $CoFe_2O_4$-added tape surface exhibited plate-like layered microstructure, which is the typical microstructure of Bi-2223 system (Figs. 5b–d). The tapes added with $CoFe_2O_4$ sintered for 100 h showed a slightly longer plate compared with the tape sintered for 50 h.

Figure 6 and Table 1 show the temperature dependence of J_c in zero magnetic fields for non-added and $CoFe_2O_4$-added tapes sintered for 50 and 100 h. The tapes with $CoFe_2O_4$ sintered for 50 and 100 h showed much higher J_c

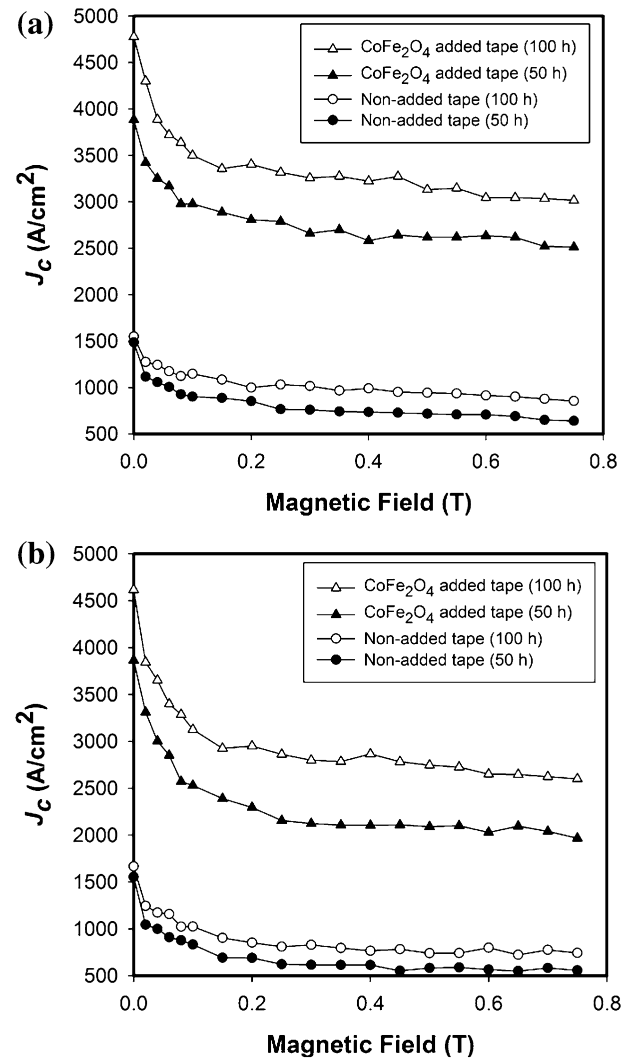

Fig. 7 Magnetic field dependence of critical current density at 77 K for non-added and $CoFe_2O_4$-added Bi-2223 tapes sintered for 50 and 100 h, in field **a** parallel and **b** perpendicular to the surface of the tape

compared with the non-added tapes. A slight increase in J_c was also observed in tapes sintered for 100 h compared with tapes sintered for 50 h. This could be due to improvement in grains connectivity with longer sintering times as seen from the longer plates in the $CoFe_2O_4$-added tapes sintered for 100 h. A higher J_c (22,420 A/cm^2 at 30 K and 4520 A/cm^2 at 77 K) was observed for tape sintered for 100 h. This value is lower compared with previous report on Ag-sheathed Bi-2223 tapes with addition of nanosized PbO sintered for 100 h (26,800 A/cm^2 and 10,700 A/cm^2 at 30 and 77 K, respectively) [15]. The higher J_c in the nanosized PbO-added sample may be due to the combined effect of enhanced flux pinning and improved microstructure that led to the significant enhancement as discussed in Ref. [15]. The improvement in microstructure is due to the relatively lower melting point of PbO.

Table 2 J_c at 30 and 77 K for Bi-2223 tapes with various nanoparticle additions

Sample	J_c (A/cm^2) at 77 K	J_c (A/cm^2) at 30 K	Ref.
Tapes			
Bi-2223 (non-added)	1290	8280	This work
$CoFe_2O_4$ (0.01 wt%) (60 nm)	4520	22,420	This work
PbO (0.05 wt%) (10–30 nm)	10,700	26,800 (40 K)	[15]
Fe_3O_4 (0.01 wt%) (40 nm)	5130	23,130	[18]
MgO (0.1 wt%) (20 nm)	3770	18,380	[21]
NiO (0.01 wt. %) (8 nm)	4500	15,530	[20]
Pellets			
Bi-2223 (non-added)	0.12	–	This work, [22]
	20	–	[4]
	8.47	–	[6]
Ag_2CO_3 (25 wt%)	30	–	[6]
Nb_2O_5 (0.10 wt%)	0.203	–	[22]
Al_2O_3 (0.20 wt%) (50 nm)	160	–	[4]
$CoFe_2O_4$ (0.01 wt%) (60 nm)	1.15	–	This work

J_c increased with a decrease in the volume fraction of the Bi-2212 phase. The presence of the Bi-2212 phase as an impurity in the Bi-2223 tapes resulted in the lowering of the zero resistance transition temperature and hence the suppression of the critical current density (Table 1).

Many applications of superconductor operate at very low fields [16]. In this work, we also studied the effect of low fields on the J_c of the tapes. Figure 7 shows J_c of the non-added and $CoFe_2O_4$-added tapes at 77 K under magnetic field applied parallel and perpendicular to the surface of the tape. J_c of $CoFe_2O_4$-added tapes sintered for 50 and 100 h was higher than the non-added tapes under applied magnetic fields. A decrease in J_c was observed under higher magnetic field strength due to the destruction of weak links in higher magnetic fields [11].

A comparison with other nanosized particle addition is shown in Table 2. A lower optimal amount (wt%) to optimize J_c was observed when the tapes are added with magnetic nanoparticles. The optimal amount of $CoFe_2O_4$ addition in this study (0.01 wt%) is similar to that of the γ-Fe_2O_3-, Fe_3O_4-, $NiFe_2O_4$- and NiO-added tapes [17–20]. For PbO- [15] and MgO [21]-added tapes, the optimal amount is $x = 0.1$ wt%. This indicated different pinning mechanisms for enhancing J_c in tapes added with magnetic and non-magnetic nanoparticles.

Samples in the pellet form also showed improvement in J_c as the samples were added with Al_2O_3 [4], Ag_2CO_3 [6], Nb_2O_5 [22] and $CoFe_2O_4$ (Table 2). Some differences in the J_c values reported by different groups may be due to the different preparation method that resulted in varied microstructure and other properties that affect the transport current. These results showed that suitable particles can be used to enhance the current density in the samples. However, J_c in the tape samples was much higher than the pellet samples as a result of the thermomechanical pressing of the tapes. Tapes added with smaller nanosized PbO (10–30 nm) and Fe_3O_4 (40 nm) showed higher J_c than the larger $CoFe_2O_4$ (60 nm)-added sample.

4 Conclusion

J_c of $CoFe_2O_4$-added Ag-sheathed Bi-2223 tapes sintered for 50 and 100 h improved significantly compared with non-added tapes. This showed that nanosized $CoFe_2O_4$ can act as effective pinning centers and enhanced the flux pinning capability of the tapes. Tapes sintered for 100 h showed a higher J_c in comparison with tapes sintered for 50 h due to improvement in grains connectivity. Therefore, a much longer sintering time is suggested to improve the transport critical current density even further. A judicious amount of magnetic nanoparticles enhanced the transport critical current density in the Bi-2223 superconductor tapes. In addition to the condensation energy associated with their core, the full vortex magnetic energy due to magnetic nanosized $CoFe_2O_4$ can contribute to J_c enhancement in Bi-2223 tapes.

Acknowledgments This research was supported by the Malaysian Ministry of Education under Grant No. FRGS/2/2013/SG02/UKM/01/1 and Universiti Kebangsaan Malaysia under Grant No. UKM-DPP-2014-055.

References

1. D. Larbalestier, Science **274**, 736 (1996)
2. D.J. Bishop, P.L. Gammel, D.A. Huse, C.A. Murray, Science **255**, 165 (1992)

3. A. Ghattas, M. Annabi, M. Zouaoui, F.B. Azzouz, M.B. Salem, Physica C **468**, 31 (1998)
4. A. Annabi, M. M'chirgui, F.B. Azzouz, M.B. Salem, Physica C **405**, 25 (2004)
5. Z.Y. Jia, H. Tang, Z.Q. Yang, Y.T. Xing, Y.Z. Wang, G.W. Qiao, Physica C **337**, 130 (2000)
6. I.H. Gul, F. Amin, A.Z. Abbasi, M. Anis-ur-Rehman, A. Maqsood, Physica C **449**, 139 (2006)
7. U. Al-Khawaja, M. Benkraouda, I.M. Obaidat, S. Alneaimi, Physica C **442**, 1 (2006)
8. N. Takezawa, K. Fukushima, Physica C **290**, 31 (1997)
9. H.L. Anderson (ed.), *A physicist's desk reference*, 2nd edn. (American Institute of Physics, New York, 1989), p. 118
10. I.F. Lyuksyutov, D.G. Naugle, Mod. Phys. Lett. B **1**(13), 491 (1999)
11. N. Sivakumar, A. Narayanasamy, K. Shinoda, C.N. Chinnasamy, B. Jeyavedan, J.M. Greneche, J. Appl. Phys. **102**, 013916 (2007)
12. M. Ismail, R. Abd-Shukor, I. Hamadneh, S.A. Halim, J. Mater. Sci. **39**, 3517 (2004)
13. Q.Y. Yu, H.K. Liu, S.X. Dou, Physica C **250**, 7 (1995)
14. R.K. Nkum, W.R. Datars, Supercond. Sci. Technol. **8**, 822 (1995)
15. N.A.A. Yahya, R. Abd-Shukor, Ceram Int. **40**, 5197 (2014)
16. E. Pardo, M. Vojenčiak, F. Gömöry, J. Šouc, Supercond. Sci. Technol **24**, 065007 (2011)
17. K.T. Lau, S.Y. Yahya, R. Abd-Shukor, J. Appl. Phys. **99**, 123904 (2006)
18. R. Abd-Shukor, W. Kong, J. Appl. Phys. **105**, 07E311 (2009)
19. W. Kong, R. Abd-Shukor, J. Supercond. Nov. Magn. **23**, 25 (2010)
20. A. Agail, R. Abd-Shukor, J. Supercond. Nov. Magn. **27**, 1273 (2014)
21. N.A.A. Yahya, R. Abd-Shukor, Adv. Condens. Matter Phys. **82**, 2013 (1073)
22. N. Ghazanfari, A. Kılıc, A. Gencer, H. Ozkan, Solid State Commun. **144**, 210 (2007)